ISSN 0965-5441, Petroleum Chemistry, 2018, Vol. 58, No. 3, pp. 250–257. © Pleiades Publishing, Ltd., 2018.

Thermal Degradation of Aviation Synthetic Lubricating Base Oil[1]

Nan Wu[a, b], Zhimin Zong[a, *], Yiwei Fei[b], Jun Ma[b], and Feng Guo[b]

[a] *Key Laboratory of Coal Processing and Efficient Utilization, Ministry of Education, China University of Mining and Technology, Jiangsu, Xuzhou, 221116 China*

[b] *Department of Aviation Oil and Material, Air Force Logistics Institute, Jiangsu, Xuzhou, 221000 China*

**e-mail: wunan_china@163.com*

Received March 17, 2017

Abstract—The thermal degradation, under oxidative pyrolysis conditions, of two synthetic lubricating base oils, poly-α-olefin (PAO) and di-ester (DE), was investigated. The main objective of the study was to characterize their behavior in simulated "areo-engine" conditions, i.e. compared the thermal stability and identified the products of thermal decomposition as a function of exposure temperature. Detailed characterizations of products were performed with Fourier transform infrared spectrometry (FTIR), gas chromatography/mass spectrometry (GC/MS), viscosity experiments and four-ball tests. The results showed that PAO had the lower thermal stability, being degraded at 200°C different from 300°C for DE. The degradation also effected the tribological properties of lubricating oil. Several by-products were identified during the thermal degradation of two lubricants. The majority of PAO products consisted of alkanes and olefins, while more oxygen-containing organic compounds were detected in DE samples according to the observation of GC/MS analysis. The related reaction mechanisms were discussed according to the experimental results.

Keywords: synthetic lubricating oil, poly-α-olefin, di-ester, thermal stability, viscosity degradation, tribological properties

DOI: 10.1134/S0965544118030179

INTRODUCTION

As the most widely used synthetic lubricating base oil, poly-α-olefin (PAO) and synthetic di-ester (DE) are formulated to suit with the automotive and industrial applications [1]. Compared to mineral oils, PAO and DE possess unique properties such as higher viscosity, lower corrosively, lower volatility and toxicity, and wider operating range [2]. The high viscosity index of PAO and DE allow these synthetic lubricants to be used under extremely hot or cold temperature, while its high mechanical and thermal stability ensures operation of equipment in severe performance applications. However, with the development of high-performance aero-engine, PAO and DE could not meet the demands of harsh terms, including the ultra-temperature, time, revolving speed and catalyst of transition metal ions, and so on [3]. In particular, viscosity thinning and color darkening of in-use oil not only embarrass the normal usage of the aero-engine, but also present the abnormal phenomenon in an instant. Hence, synthetic aviation lubricating oil (SALO) must be replaced frequently to match the high performance demands. In comparison to the non-degraded lubricant oils, more micro-molecules and other organic matters are included in the degraded ones, which influence lubricants' comprehensive properties severely, such as lubricity, viscosity and volatility [4]. For this purpose, understanding molecular composition of organic matter in in-use SALO is crucially important.

The determination of lubricant application associated with the degradation processes is an interesting topic of research. Many studies have described how the molecular composition of base oil influences its physical and chemical properties, especially its thermal stability which is connected to both the initial temperature and the rate of degradation of polymers [5–13].

Significant advances in analytical instrumentation have given a big boost to the process of detecting lubricants. For example, as a commonly used instrument, gas chromatography/mass spectrometer (GC/MS) is effective for analyzing some volatile species by passing test fluids over oil-coated chromosorb packed in GC column and measuring the retentions index to monitor oil degradation, through which we could monitor the thermal-oxidative stability of lubricants. GC/MS has been successfully applied in many fields [14–17], however, to the best of our knowledge, few studies on ther-

[1] The article is published in the original.

Table 1. Typical pproerties of PAO

Properties	PAO	Test Method
Kinematic viscosity (40°C)/(mm^2/s)	17.94	ASTM D445
Kinematic viscosity (100°C)/(mm^2/s)	4.018	ASTM D445
Viscosity index	131	ASTM D2270
Flash point(COC)/(°C)	201	ASTM D92
Pour point/(°C)	<–68	ASTM D97
Acid number/(mg KOH/g)	0.009	ASTM D974

mal-oxidation of lubricants and their derivatives covered the application of this technique.

Both PAO and DE are typical synthetic lubricating base oils in China and were extensively investigated [9, 13, 18–22]. Nevertheless, more investigations are needed to probe the complex chemical changes using analytical techniques including a number of spectroscopic studies such as ultraviolet (UV), infrared (IR) and GC/MS. In the present study, structural features of PAO, DE and their reacted samples were characterized by traditional viscosity experiment and analyzed with GC/MS. Influence of degradation products on the tribological properties of PAO and DE was also discussed.

EXPERIMENTAL

Oil Sample and Reagents

PAO and Di(2-ethylhexyl)adipate (DOA) (a kind of DE) were collected from Air Force Fuel Research Institute. The typical properies of PAO were shown in Table 1. Petroleum ether (90–120°C), acetone and n-hexane used in the experiments were analytical reagents, and all the organic solvents were distilled before use with a Büchi R-210 rotary evaporator.

Thermal Degradation Experiments

Both PAO and DOA were heat-treated at 170, 200, and 300°C, respectively, in a 500 mL stainless-steel, magnetically stirred autoclave with the stirring rate of 800 r/min. After reaction for 2 h, the reacted samples were withdrawn at room temperature. And then, the kinematic viscosity (KV) and total acid number (TAN) of the reaction product were measured according to ASTM D445 and ASTM D974 respectively. For convenience in description, the PAO, DOA, and their oxidized samples under 170, 200, and 300°C were abbreviated as P_0, P_1, P_2, P_3 and D_0, D_1, D_2, D_3, separately.

Analytical Methods

PAO, DOA and their degraded samples were analyzed with a Nicolet Magna IR-560 Fourier transform infrared (FTIR) spectrometer by collecting 32 scans at a resolution of 4 cm^{-1} in reflectance mode with measuring region of 4000–400 cm^{-1}.

Afterwards, oil samples were analyzed with a Hewlett-Packard 6890/5973 GC/MS, which was equipped with a capillary column coated with HP-5MS (crosslink 0.5% PH ME siloxane, 60 m length, 0.25 mm inner diameter, 0.25 m film thickness) and a quadrupole analyzer with a m/z range from 33 to 500 and operated in electron impact (70 eV) mode. The capillary column was heated from 120 to 274°C at a rate of 13°C min^{-1} and held for 2 min, then raised to 281°C min^{-1} at a rate of 0.5°C min^{-1} and held for 2 min, finally raised to 300°C at a rate of 12°C min^{-1} and held at 300°C for 3 min. Data were acquired and processed using software of Agilent MSD Productivity Chemstation. Compounds were identified by comparing mass spectra with NIST05a library data.

And using MQ-800 four-ball tester produced by Jinan Testers Factory to evaluate the wear and friction characteristics of degradation samples with the conditions of rotating rate 1450 r/min, test duration 30 min, and load 392N. The balls used in the tests were made of GCr 15 (AISI 52100) bearing steel with HRC 59-61. The wear scar diameters (WSDs) were measured by using an optical microscope. Parallel experiments were done to ensure the relative error less than 5%.

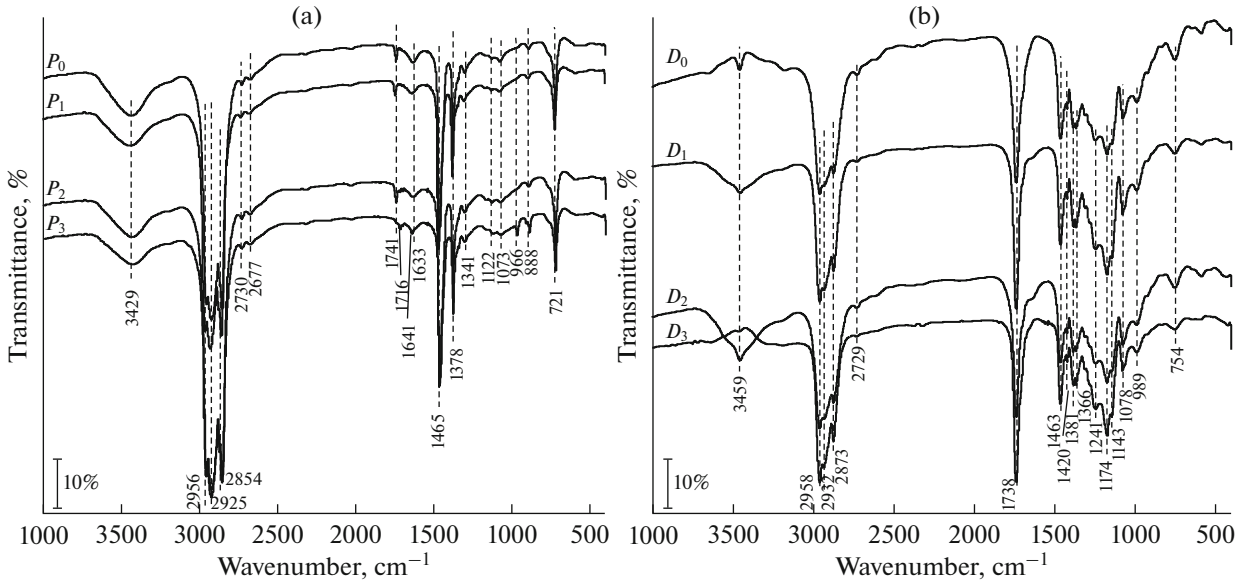

Fig. 1. Infrared spectra of PAO (a), DOA (b), and their reacted samples.

RESULTS AND DISUSSION

FTIR Analysis

During thermal degradation, synthetic lubricant oils may go under changes in compositions. Products, which are harmful to the high-performance of these oils, may be formed due to cracking process, changing its properties [23].

Obvious differences in the FTIR spectra among PAO and DOA and their reacted samples can be observed from Fig. 1. The absorbance of aliphatic moieties (AMs) from P_n (n = 0–3) around 2850–2960 cm^{-1} and 1465 cm^{-1} are much stronger than those from D_n, indicating that AM-rich species in P_n are predominant products, which could be ascribed to the special structure of PAO, multi-aligned comb-likely side-chains and skeleton bones of straight chain alkynes, too. The stretching vibration of –OH group around 3429 and 3459 cm^{-1} from D_n is much stronger than from P_n, which suggesting that species containing –OH were produced in D_n. The weak absorbance around 1641, 1633, 966, and 888 cm^{-1} are assigned to C=C bending vibration, indicating that olefins may exist in P_3.

Remarkably stronger absorbance at 1738 cm^{-1} assigned to –C=O bond of carboxyl groups in D_n than that in P_n proved that esters are dominating compounds. The characteristic absorbance of the carbonyl group form aldehydes, ketones and carboxylic acids is around 1716 cm^{-1}. Such absorbance from P_3 is very weak, suggesting that fractional substances are oxygenized. The absorbance of more $-(CH_2)_n-$ at 754 cm^{-1} of D_3 is appreciably stronger than that in D_0, which indicates that DOA has been pyrolysis under thermal conditions.

GC/MS Analysis

There are 101 micro-compounds (MCs) were identified from P_n (n = 0–3) by GC/MS analysis, including 13 n-alkanes (NAs), 26 isoparaffins (IPs), 51 olefins (OFs), and 11 other compounds (OCs). While for DOA samples, there are 53 MCs were determined, including 24 single esters (SEs), 13 micro-di-esters (MDEs), 9 ketones, 1 alkane, 2 ethers, 1 organic acids (OAs), and 3 alcohol.

As illustrated in Fig. 2a, NAs, IPs and OFs are main products from pyrolysis of PAO. The range of carbon number in NAs is from 12 to 24 and eicosane is predominant individual component. The relative content (RC) of OFs is equivalent to that of NAs and carbon number is from 12 to 23, implying that further molecular recombination happened in the pyrolysis condition. This result is in agreement with the molecular composition of PAO, less oxygen-containing organic compounds (OCOCs), but a high content of long-chain macromolecular species. The detection of OCOCs is in consistent with FTIR analysis stated above. However, RC of OCOCs is 1.02% and all of them only appeared in P_3. As we all know, RC of OCOCs represents the oxidation degree of PAO and it is obvious that breakage rather than oxidation is dominantly under thermal atmosphere, as depicted in Scheme 1.

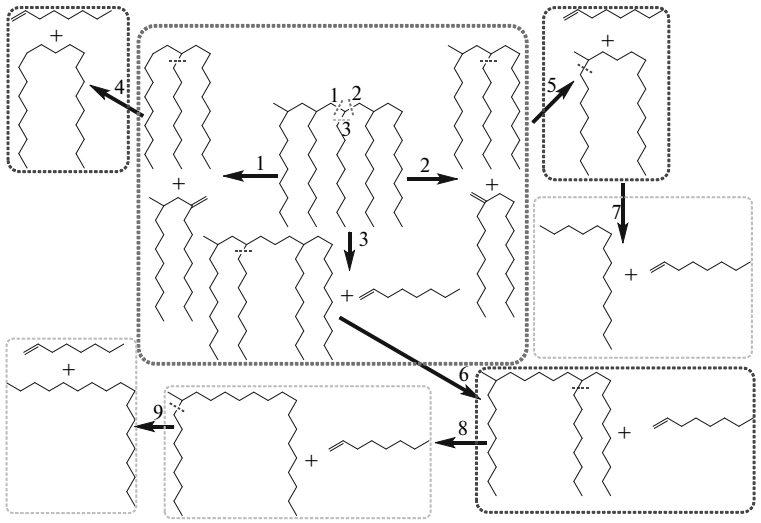

Scheme 1. Mechanism for the oxidative pyrolysis reactions of PAO.

PAO first broke weak covalent bonds such as $-CH_2-$ bonds to produce large amounts of MCs and then some of them gradually rearranged by further reaction to afford OFs. According to the supposition, the formation of NAs and/or IPs could be ascribed to the cleavage of weak covalent bonds at the tertiary carbon atom.

Further decomposition of OFs and OCOCs can consequently lead to the formation of di-alkenes or vinyl radicals vial dehydrogenation. However, at temperatures higher than 300°C, such dialkenes and vinyl radicals are efficiently destroyed leading to a very small benzene production, which makes the oils color deepened.

As Fig. 2b exhibits, the RC of SEs decreases in the order: $D_3 \gg D_2 > D_1 > D_0$. RC of SEs from D_3 (1.35%) is triple more than that from D_2 (0.49%), whereas SEs in D_1, D_2, and D_3 are mainly short-chain species with carbon number from 13 to 16, indicating that the thermal rupture dramatically increased the yields of short-chain SEs. In addition, there are few significant differences in the RC of MDEs (0.25%), ketone (0.12%), OAs (0.018%), ether (0.005%) and alcohol (0.05%) between D_1 and D_2, but much lower than that from D_3. 6-(2-ethylhexyloxy)-6-oxohexanoic acid is predominant in OCOCs from D_3 with 0.02% of RC, which is related to the fact that the acid value of D_3 is 12.597 mg

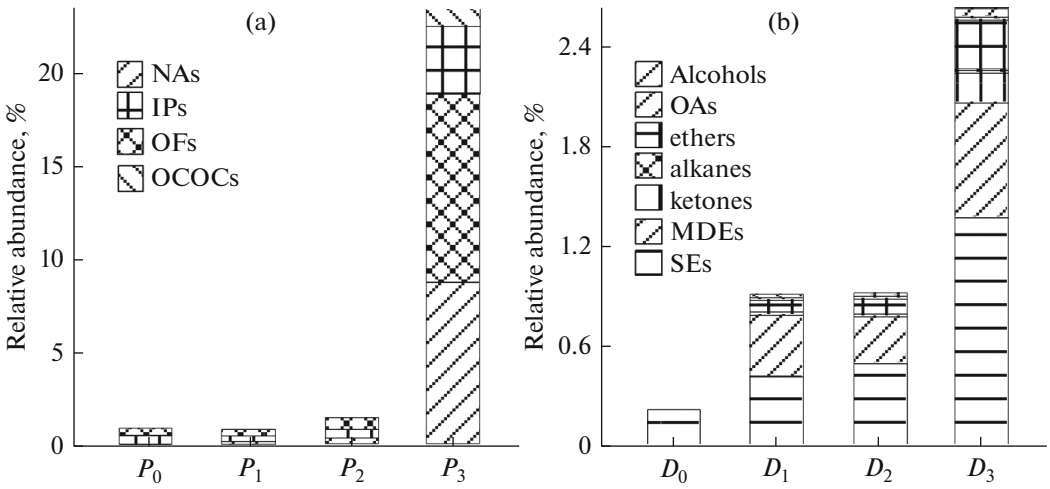

Fig. 2. Relative abundance of reacted samples of PAO (a) and DOA (b).

KOH/g, much higher than that of P_3. 2-Cyclopentenylethenylpentanone is the most abundant in ketone from D_1, D_2, and D_3, contributing to the deepened color in reacted samples.

The formation of OCOCs from DOA could be explained that under high temperature conditions the O–C bond is likely to rupture after the formation of hydrogen peroxide, and then giving rise to format a phenyl radical. This radical can, in turn, be quenched by a hydrogen atom leading, finally, to the formation of chromophore in large quantities. The higher OCOCs production of DOA compared to that of PAO may be due to the different chemical composition of the two samples.

In addition, as demonstrated in Fig. 3, 7 OCOCs were confirmed in the products from DOA degradation. Various compounds were identified from oil oxidation, but to our knowledge, few reports have been issued on the detection of OCOCs in the products from DOA degradation. Compared to those obtained under pyrolysis conditions (where a plateau of benzene formation was obtained at temperatures higher than 300°C for all lubricants), the results clearly show the positive effect due to the presence of oxygen, leading to the formation of reactive oxygenated species. This results in oxidation reactions of both benzyl and alkyl radicals which, ultimately, give rise to the observed increase in OCOCs formation at higher temperatures. This again reflects a different formation mechanism that has to proceed, as already mentioned, via the intermediate formation of ketone by means of dialkenes and vinyl radical displacement and cyclization reactions.

Ketone, then, may further polycondense and polymerize with the same radicals giving rise to aromatic radicals that, acting as building blocks, generate heavy species by consecutive reactions and, eventually, to highly condensed groups (non-volatile) that are included into the black char deposit.

However, these compounds do not represent the totality of by-products formed because at the end of the test, i.e. after the experiments at high temperature, there is evidence of a light black solid deposit (char) left in the samples, probably due to high molecular weight (or polymerized) compounds. It is not possible to characterize the compounds responsible for forming this solid deposit because the analytical technique employed (GC/MS) only allowed volatile and semi-volatile by-products to be detected.

Viscosity Analysis

In general, oils high in long straight-chained content and certain sulfur and nitrogen containing species exhibit faster degradation. Nowadays, KV is often used to predict actual lubricant service life in high temperature and other extreme applications. Noteworthy, the more resistant a lubricant is to thermal-oxidation, the fewer tendencies it has to viscosity increases during use [3].

The thermal stability profiles of the PAO and DOA can be depicted in Fig. 4, each point representing the viscosity of degraded oils respectively. From this figure, viscosity for the two synthetic lubricants follows the order PAO > DOA, which might be corresponding to the fact that PAO has a higher content of long-chain AMs than DOA. However, PAO has the lower thermal stability and its degradation starts at temperatures lower than 200°C, with 23.8% of RC in MCs. DOA, in fact, is made of OCOCs being constituted of methyl and ethyl di-ester, which makes it more thermal stable than PAO with a high NAs content. In addition, the higher thermal stability of DOA, with respect to PAO, can be attributed to the higher content of stable species which is quiet a resistant compound thermally.

Total Acid Number (TAN) Analysis

Acid value is often used to measure the corrosive properties of lubricating oil. The high TAN will accelerate corrosion and shorten the service life of the engine. It can be seen from Fig. 5 that TAN of PAO base oil and its high temperature reaction samples increased with the temperature going up. When the temperature was higher than 200°C, the acid value increased sharply, but still at a low level. Even if the temperature rose to 300°C, the acid value was only 0.493 mg KOH/g. Meanwhile, TAN of DOA and its tested samples had the similar trend, but the values were higher comparing with PAOs. TAN of the DOA tested oil at 200°C raised to1.568 mg KOH/g, which can cause serious corrosion to the engine lubrication system. From 200 to 300°C, the TAN increased by 11.029 mg KOH/g to 12.597 mg KOH/g, indicating that the oil sample had been seriously deteriorated. The difference between the two SALO can be attributed to the fact that the ester lubricating oil produces more acidic substances after high temperature oxidation and increases the acid value.

Wear and Friction Performance Analysis

Figure 6 showed the variation of WSDs with temperature of PAO and DOA oxidation products. It can be seen that the WSDs of the oil oxidation products reached maximum values of 1.10 mm to PAO oxidation products, and 0.79 mm to DOA oxidation products, respectively. It may be due to a large number of small molecules produced by the high temperature oxidation, which weakened the anti-wear properties of oil and damaged the friction surface seriously. With the increasing of temperature, the WSDs of PAO and DOA oxidation products decreased, but still higher than that of non-oxidized oil, which indicated the oxi-

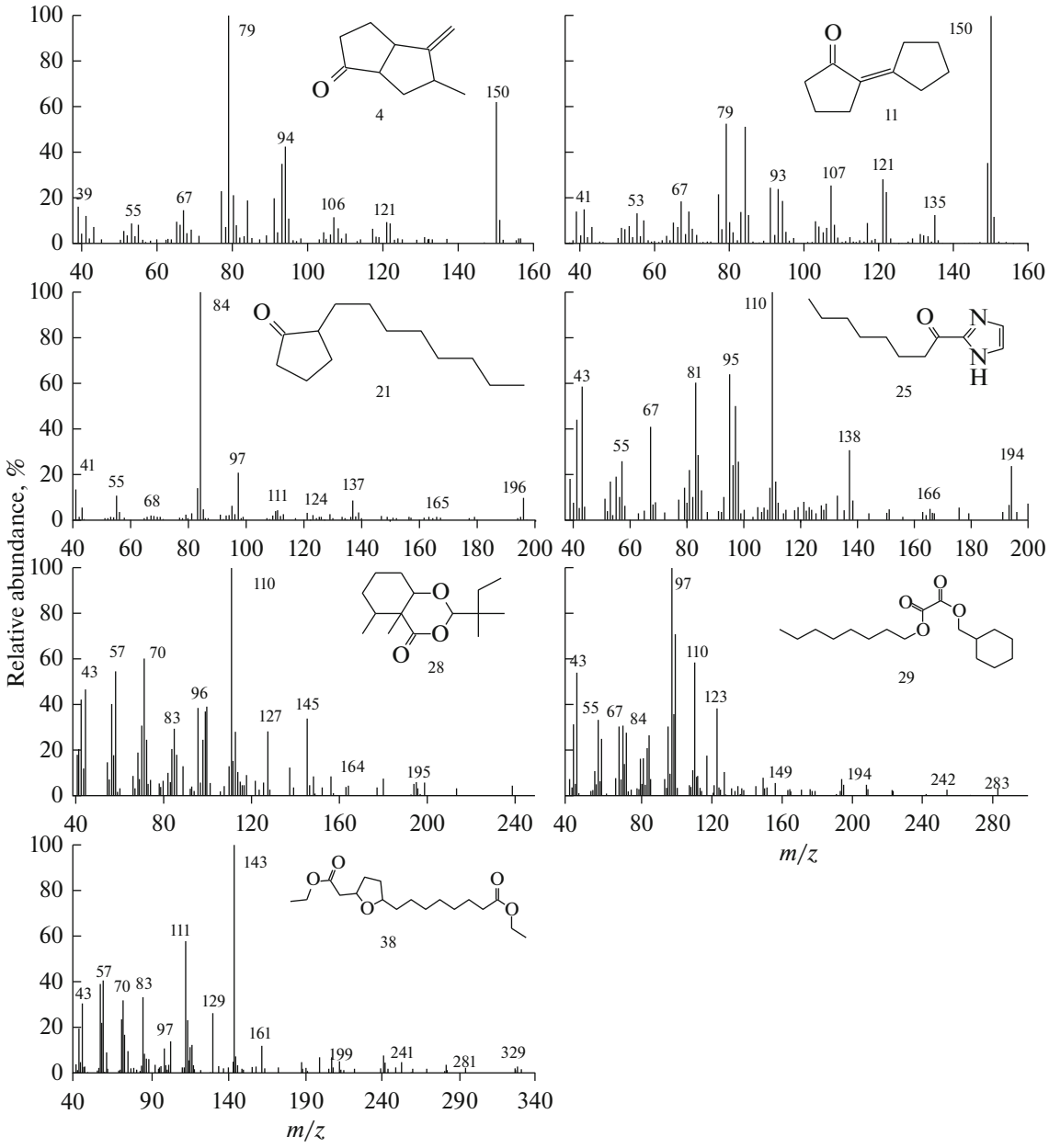

Fig. 3. Mass spectrums of some chromophore detected from DOA oxidized samples.

dation temperature had a great effect on the anti-wear properties of synthetic lubricants. And under the same conditions, PAO oxidation products had larger WSDs than DOAs, which may be due to formation of the acidic substances produced during the oxidation process to improve the friction and wear resistance of the lubricating oils.

CONCLUSIONS

Thermal treatments along with subsequent products separation and analyses prove to be effective approach for understanding the pyrolysis of PAO and DOA. According to the investigations, NAs, IPs and OFs are important moieties and short-chain AMs are predominant in P_1, P_2, and P_3. The products from thermal degradation in DOA are rich in SEs, MDEs, ketone, ether, OAs, and alcohol, which leads to higher acid value than that of PAO reacted samples. Viscosity experiment is expected to be an effective method for inquiring degradation extent of aero-engine lubricants. The significant decrease of viscosity in PAO reveals its lower thermal stability compared to DOA. The small molecules formation in the thermal degra-

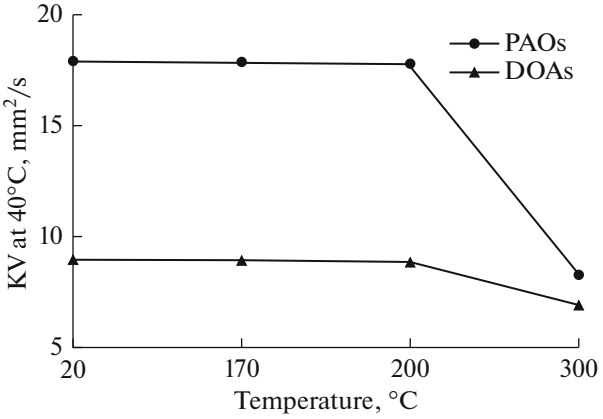

Fig. 4. Variations in KV values (40°C) with temperature of PAO and DOA tested samples.

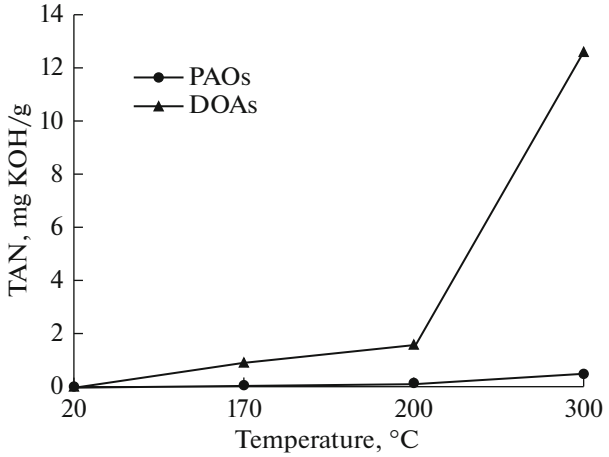

Fig. 5. Variations in TAN values with temperature of PAO and DOA tested samples.

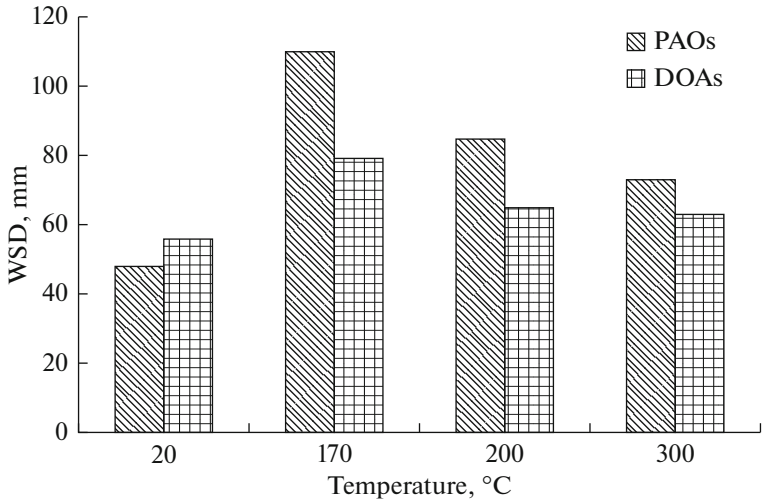

Fig. 6. Variations in WSDs with temperature of PAO and DOA tested samples.

dation would sihnificantly affected tribological properties of PAO and DOA.

ACKNOWLEDGMENTS

This work was subsidized by the Jiangsu Provincial Natural Science Foundation of China (Grant BK20161187), Xuzhou Science and Technology Development Funds (Grant KC16SG269), and a Project Funded by the Priority Academic Program Development of Jiangsu Higher Education Institutions.

REFERENCES

1. G. J. Bishop, Lubr. Sci. **4**, 25 (1987).
2. L. I. Kioupis and E. J. Maginn, J. Phys. Chem. B **103**, 10781 (1999).
3. B. K. Sharma and A. J. Stipanovic, Thermochim. Acta **402**, 1 (2003).
4. E. Beran, Tribol. Int. **43**, 2372 (2010).
5. J. Yao and J. Dong, Thermochim. Acta **262**, 157 (1995).
6. D. Du, S. Kim, W. Moon, S. Jin, and W. Kwon, Thermochim. Acta **407**, 17 (2003).
7. B. N. Barman, Tribol. Int. **35**, 15 (2002).
8. S. M. Powell, I. Snape, J. P. Bowman, B. Thompson, and J. S. Stark, J. Exp. Mar. Biol. Ecol. **322**, 53 (2005).
9. G. Mascolo, R. Rausa, G. Bagnuolo, G. Mininni, and L. Tinucci, J. Anal. Appl. Pyrol. **75**, 167 (2006).
10. J. Zhu, W. Liu, R. Chu, and X. Meng, Tribol. Int. **40**, 10 (2007).

11. S. H. P. Bettini, M. P. P. de Miranda Josefovich, P. A. R. Muñoz, C. Lotti, and L. H. C. Mattoso, Carbohyd. Polym. **94**, 800 (2013).
12. M. Kotera, Y. Urushihara, D. Izumo, and T. Nishino, Thermochim. Acta **531**, 1 (2012).
13. J. E. Martín-Alfonso, C. Valencia, and J. M. Franco, Polym. Test. **32**, 516 (2013).
14. M. Commodo, I. Fabris, C. P. T. Groth, and O. L. Gülder, Energy Fuel **25**, 2142 (2011).
15. X. Fan, X. Y. Wei, and Z. M. Zong, Fuel **109**, 28 (2013).
16. Z. Li, X. Wei, H. Yan, and Z. Zong, Fuel **153**, 176 (2015).
17. F. C. Wang and W. C. Buzanowski, J. Chromatogr. A **891**, 313 (2000).
18. S. D. Kouame and E. Liu, Tribol. Int. **72**, 58 (2014).
19. J. Hu, X. Wei, J. Yao, L. Han, and Z. Zong, Tribol. Int. **39**, 1469 (2006).
20. M. Diaby, P. Singhal, M. Ousmane, M. Sablier, A. Le Négrate, M. E. Fassi, and V. Zymla, Fuel **107**, 90 (2013).
21. M. J. Yanjarappa and S. Sivaram, Prog. Polym. Sci. **27**, 1347 (2002).
22. G. Dlubek, D. Bamford, O. Henschke, J. Knorr, M. A. Alam, M. Arnold, and Th. Lüpke, Polymer **42**, 5381 (2001).
23. S. Amat, Z. Braham, Y. Le Dréau, J. Kister, and N. Dupuy, Talanta, **107**, 219 (2013).